Research Square

Preprints are preliminary reports that have not undergone peer review.
They should not be considered conclusive, used to inform clinical practice,
or referenced by the media as validated information.

Comparative evaluation of the shielding capacities between space suits made from the composite material ABnC on planetary bodies

Lasany Arfin Kunja
Chungnam National University
Yu Yi
euyiyu@cnu.ac.kr

Chungnam National University
Eojin Kim
Korea Astronomy and Space Science Institute
Jongdae Sohn
Korea Astronomy and Space Science Institute
Jonggil Jung
Korea Astronomy and Space Science Institute

Article

Keywords: Space Suit Shielding, ABnC materials, GCR, Neutron shielding, Monte Carlo Simulations, Radiation shielding

Posted Date: November 27th, 2026

DOI: https://doi.org/10.21203/rs.3.rs-11706421/v1

License: This work is licensed under a Creative Commons Attribution 4.0 International License.
Read Full License

Additional Declarations: No competing interests reported.

Abstract

The Moon and Mars are the primary targets for future human exploration outside of Earth and are also among the most likely places for future human habitation. Extreme radiation is a significant barrier to human settlement. Galactic cosmic radiation, solar particles, and albedo radiation events have been detected in free space and on the surfaces of planets and moons. Unlike Earth, the Moon and Mars do not provide any protection for a potential secure zone because of their weak magnetic fields and extremely thin atmospheres. In this study, we investigated the radiation shielding properties of possible materials for space suits. In addition to conventional materials, we investigated an AB_n composite made from Aromatic Amide Polymer (A) and Boron Nitride nanotubes (B). This composite material can be spun into fibers and made into textile materials to be utilized in space suits. We performed Monte-Carlo simulations in MULASSIS (Multi-Layered Shielding Simulation Software) to test the shielding efficiency of AB_nC against various contributions of GCR and secondary radiation, and compare it against traditional materials. We found that A, which is rich in hydrogen, worked best for most radiation types, including fast secondary neutrons, while AB_5C, which is rich in boron, provides the best shielding qualities against thermal neutrons.

INTRODUCTION

Planetary bodies like the Moon and Mars lack an Earth-like atmosphere and a powerful magnetic field; as a result, they have extremely high radiation levels. Cosmic radiation is one of the main things endangering the health of astronauts[1]. Alpha, Beta, and gamma radiation, which stand for Helium nuclei, Electrons or Positrons, and Photon radiation, are also active in space radiation. Despite being visible on Earth, alpha particles are often only associated with radioactive decay. Like their less energetic cousins, X-rays and gamma rays are high-energy electromagnetic radiation [2]. These radiations originate from secondary radiation and GCR. Despite the small number of cases, secondary radiation poses a significant health risk to astronauts. According to our understanding, it can cause both malignant and non-cancerous health problems. This is why GCR, as well as secondary radiation, must be taken into consideration. The main radiation health risks for astronaut crews on exploration missions are cancer, genetic anomalies, and degenerative vascular changes [3].

Potential shielding materials for deep space missions are being investigated, including polymers, liquid gas, hydride, silica, lead, aluminium, and various composite materials [4]. Previous research additionally looked at the use of aluminium, water, and polyethylene as radiation shielding materials on the surface of planetary objects. Furthermore, certain materials among them may contain water [5], including CFRP (Carbon-Fiber Reinforced Polymer), resins [6 7]. The possibility of towels and sanitary towels as shielding has been studied. Hydrogen-rich materials play a vital role in radiation shielding [8]. LiH (Lithium Hydride) has been acknowledged as a superior shielding agent as well [9 10].

To make space suits, some conventional materials have traditionally been used to lower the radiation level below health risks. However, for astronauts' health, some of them, like Mylar or other conventional materials, have not proved to be very effective. These conventional materials are primarily made of Aluminium, Rubber, Teflon, Nylon, and Mylar, among others. The majority of these materials have been utilized in space suits during shorter-duration space missions, such as Apollo missions on the Moon [11]. Because of their historical use in radiation shielding in the space, we have chosen Nylon, Mylar, and Al for our candidates as traditional materials. We may need to switch from traditional materials to different composite materials that contain both hydrogen and boron in order to improve the shielding materials for space suits. Because hydrogen-rich materials can scatter high-energy particles through continual collisions and transform them into low-energy particles that have minimal penetrating capabilities, they have long been utilized in radiation shielding [12].

A newly developed substance that contains both hydrogen and boron, but in varying proportions in each version, has been introduced [13]. We can better understand which combination is best for certain types of radiation by considering the proportion of hydrogen and boron. Six distinct variations were obtained: A, AB_1, AB_2, AB_3, AB_4, and AB_5. A has the most hydrogen and no boron, but the percentage of boron rises with the other variations, and the percentage of hydrogen decreases and reaches its minimum in AB_5.

Monte-Carlo simulations, including GCR and albedo radiation, were used in the simulation to evaluate the shielding efficiency of the chosen materials. The GEANT-4 (Geometry and Tracking)-based SPENVIS (Space Environment Information System)[14] incorporates MULASSIS [15] to perform those simulations [16].

DATA AND METHOD

Radiation models

GCR are composed of energetic particles with a broad range of mass and energy values. Roughly 2% are referred to as heavy nuclei of HZE particles (high atomic number and energy) or other ions, whereas 98% are lighter nuclei. [17]. A broad characterization of space radiation has been produced using several simulations, including GEANT-4, since it is very difficult to duplicate the free space radiation or radiation environment on planetary bodies such as the Moon and Mars in a laboratory setting [16]. This approach of a simulated radiation environment was employed in the present study. Numerical data were extracted from the graphical plots using WebPlotDigitizer.

Software Settings

The "standard electromagnetic" (EM) physics packages were utilized in MULASSIS (v1.23) for SPE, low-energy electromagnetic (LEEM) processes, and GCR computations. GEANT-4 is a Monte Carlo particle transport toolkit that incorporates a wide range of physics models for simulating radiation–matter interactions. As a GEANT-4-based application, MULASSIS employs these physics models to perform

radiation shielding analyses. Depending on the selected incident particle and radiation environment, MULASSIS automatically applies the appropriate physics configuration. The QBBC physics list is from GEANT-4, employed to account for electromagnetic and hadronic interactions. We used linear interpolation based on the simulation parameters and set the incident angle to 0.0. "Parallel beam" was selected for angular distribution from the simulation setup for all radiation, including GCR and albedo radiation. The source particle energies were introduced into the software in a tabular form as energy (MeV) – flux (cm^{-2} MeV^{-1} s^{-1}) data, according to the spectra shown in Figs. 1 and 2. For activities below a few keV, the low-energy package is more accurate than the normal package. [21]. Monte Carlo (M-C) simulation, a sophisticated and computationally demanding technique, is used to simulate particle motion. GEANT-4 is regarded as a very useful toolkit for M-C simulations of low-energy electron and photon sources. [16]. For low-energy radiation sources, the inaccuracy in the shielding efficiency of the materials that MULASSIS simulates can be around 6%.

Modelling and Materials

The materials we chose are from the reference [13] and are sorted in Table 1. We know hydrogen and boron contribute to radiation shielding very differently. While hydrogen attenuates the radiation and scatters it, resulting in low-energy radiation, on the other hand, boron has the highest thermal neutron $_{ab}$sorption cross section. Because of their different natures in acting towards different types of radiation, materials rich in hydrogen and materials rich in boron are meant to act differently towards different types of radiation. Our chosen material contains both hydrogen and boron, but different variants contain different proportions of hydrogen and boron, making it suitable for different kinds of radiation.

Table 1
Properties of the materials used in the simulations, showing the chemical formula (~ 100 atoms per formula unit), density, and atomic percentages of boron and hydrogen in the AB_nC materials. The densities are taken from [13].

Material and Chemical Composition	Density (g/cm^3)	Percentage of Boron	Percentage of Hydrogen
A (C50 H36 N7 O7)	1.40	0	36
AB_1C (C45 H32 N11 O6 B5)	1.42	5	32
AB_2C (C40 H29 N16 O6 B10)	1.47	10	29
AB_3C (C35 H25 N20 O5 B15)	1.51	15	25
AB_4C (C30 H22 N24 O4 B20)	1.67	20	22
AB_5C (C25 H18 N29 O4 B25)	1.80	25	18

Materials containing hydrogen provide the best protection against most kinds of radiation, including fast neutron radiation. In our suit materials, the hydrogen content is essential for shielding against secondary (fast) neutron radiation as is boron for shielding from thermal neutrons.

Table 2
Properties of the materials used in the simulations, showing the chemical formula (~ 100 atoms per formula unit) and density of the materials

Material and Chemical Composition	Percentages of Boron	Density (g/cm^3)	Percentage of Hydrogen
Mylar	0	1.39	36
Aluminium	0	2.7	0
Nylon	0	1.14	58

Simulation Set-up

Due to various modeling restrictions of the simulation environments, it was not possible to examine radiation in all types of structural designs. Slab models, where flat layers of material are arranged on top of one another, are available in MULASSIS. Thus, in the MULASSIS simulations, a shielding model with slabs was employed.

As our simulated model system of MULASSIS, we layered a slab of the AB_nC or traditional space suit material with an areal density of 0.41 mg/cm^2 on top of a 1.5 mm thick layer of skin (see Fig. 3). Because different AB_nC or traditional materials have different densities and a fair comparison of the materials must be made, areal densities have been used in place of thicknesses. The outcome should not be interpreted as a thickness comparison, but rather as a mass per area comparison. The shielding effectiveness of the chosen material is calculated according to the radiation absorbed in the skin layer underneath the material. A lower absorbed dose in the skin layer means, therefore better shielding by the testing material.

Since the absorbed dose indicates the real amount of energy deposited in the target, it has been selected as the analytical parameter in MULASSIS. It is measurable in several materials. The absorbed dose makes biological impacts simple to comprehend.

RESULTS

Shielding behavior of AB_nC materials

These simulations using MULASSIS / GEANT-4 contained a slab model with a 410 µg/cm^2 slab of AB_nC materials of varying areal densities of the chosen material. Overall, different outcomes are observed, showing a dose reduction with increasing areal densities of materials for both galactic cosmic rays in space (see Fig. 4) and on the Martian surface (see Fig. 5). The result should be seen as a comparison of mass per area rather than thickness. All the absorbed radiation dose was measured on 1.5 mm of skin. The lower dose of absorption indicates better shielding capability.

The simulations also offer an understanding of the comparative shielding performance of the different combinations of AB_nC materials that are rich in hydrogen and boron. For different types of GCR (Fig. 4), each material shows distinct shielding performance. The general order of shielding performance is A > AB_1 > AB_2 > AB_3 > AB_4 > AB_5. A shows the best shielding capacity in the AB_nC family, and AB_1C performed best among all AB_nC materials that contain boron.

For the GCR on the Martian surface (Fig. 5), the shielding performance of all materials follows the same trend as for the GCR space radiation. The order of performance for the different materials is again A > AB_1 > AB_2 > AB_3 > AB_4 > AB_5.

For the secondary Neutron and Gamma radiation on the lunar surface (Fig. 6), the shielding performance of all materials follows the same trend as for the GCR space radiation. The order of performance for the

different materials is again A>AB_1>AB_2>AB_3>AB_4>AB_5. A shows the best shielding capacity in the AB_nC family, and AB_1C performed best among all AB_nC materials that contain boron.

Overall, in both space and on the Martian surface for GCR and secondary radiation, A shows the highest shielding performance, while AB_5 shows the lowest as a shielding material. The results of this paper validated our earlier conclusion based on different simulations that the optimum materials for shielding on the lunar surface are those that are rich in hydrogen [9 108].

Thermal neutrons are low-energy neutrons that have slowed down to thermal equilibrium with the surrounding material, whereas secondary neutrons are newly produced high-energy neutrons generated by nuclear interactions of primary radiation with matter. For secondary neutron radiation from Fig. 7, A shows the highest shielding performance, while AB_5 shows the lowest as a shielding material. On the other hand, only for thermal neutron radiation, the order of performance is opposite: A<AB_1<AB_2<AB_3<AB_4<AB_5. Fast secondary neutrons are absorbed or scattered by the shielding materials, thereby slowing them down. For this reason, hydrogen-rich materials exhibit greater shielding against secondary neutrons. On the other hand, boron has a larger thermal neutron absorption cross-section, and boron-rich materials perform better in shielding from thermal neutrons. The results of this paper validated our earlier conclusion based on different simulations that the optimum materials for shielding on the lunar surface are those that are rich in hydrogen.

It needs to be mentioned that Neutron shielding results are simulated using energy-grouped input radiation for fast and thermal neutrons, without explicit energy-dependent weighting. Therefore, the results represent energy group-wise shielding behavior rather than a complete evaluation of total neutron dose based on the full energy spectrum. Additionally, the AB_nC materials were modeled as homogeneous slabs, without incorporating layered moderator or absorber configurations.

For the secondary Neutron radiation on the lunar surface (Fig. 8), the shielding performance of two AB_n composite materials was compared with traditional shielding. The order of performance for the different materials is again Nylon > A>AB_5C > Al>Mylar. Overall, secondary Neutron radiation shows that AB_nC materials are in the middle in radiation shielding parameters compared to traditional materials. Although it needs to be mentioned that the result from Fig. 8 has been limited to a single secondary neutron radiation environment on the lunar surface. It does not cover the full spectrum of space radiation.

This manuscript's results are a comparative study of different materials with the same areal densities rather than the direct use for engineering a layer on a space suit with the same areal densities or thickness that we simulated.

DISCUSSION

The garment made with Aromatic Amide Polymer and boron Nitride of different varieties of hydrogen and boron contents showed different shielding properties towards different radiations. For most of the

radiations, including fast secondary neutrons, materials rich in hydrogen are better for shielding. Only for thermal neutrons, materials high in boron percentage worked better than hydrogen-rich materials. The reason for this behavior is that high-energy neutrons can be most efficiently scattered by hydrogen atoms. For the slow thermal neutrons, however, the large neutron absorption cross section of the boron nuclei is the critical factor, leading to a better shielding efficiency for thermal neutrons.

A is the best-performing material in the AB_n composite materials family to shield against all radiation implemented in the manuscript, except for thermal neutron radiation. AB_1C performed better than all other AB_n composite materials containing boron, especially AB_5C. Containing a higher percentage of hydrogen made AB_1C more effective for most radiation, including secondary fast neutrons. For thermal neutrons, AB_5C performed better than all other AB_n composite materials because of the higher boron concentration. It can be said that whereas hydrogen-rich materials from the AB_n composite materials family showed strong shielding capability against GCR, secondary fast neutrons, and secondary gamma, boron-rich materials worked best for thermal neutron shielding. However, none of these composite materials exhibit a significant improvement or deterioration in performance compared to traditional materials like Nylon or Mylar.

Declarations

Acknowledgements

L.A.K. acknowledges financial support from the Brain Korea 21 scholarship. This research was supported by the National Research Foundation of Korea (NRF-2022R1A2C1092602). Furthermore, this research was supported by the Global Learning & Academic Research Institution for Master's, PhD students, and Postdocs (G-LAMP) Program of the National Research Foundation of Korea, funded by the Ministry of Education (No. RS-2025-25442707).

Author Declaration

Conflict of Interest

The authors have no conflicts to disclose.

Author Contributions

Lasany Arfin Kunja: Formal Analysis (lead); Visualization (lead): Methodology (lead); Writing - original draft (lead), Review and Editing (equal). **Yu Yi:** Funding Acquisition (lead); Project Administration (lead); Review and Editing (equal); Supervision (Equal); Resources (lead). **Eojin Kim**: Review and Editing (equal); Supervision (equal). **Jongdae Sohn:** Review and Editing (supporting); Supervision (supporting). **Jongil Jung**: Review and Editing (supporting); Supervision (supporting).

Data Availability

The data that support the findings of this study are available within the article.

References

1. Cucinotta, F. et al. Space Radiation Cancer Risk Projections for Exploration Missions: Uncertainty Reduction and Mitigation. (2001).
2. Freese, S., Reddy, A. P. & Lehnhardt, K. Radiation impacts on human health during spaceflight beyond Low Earth Orbit. *REACH* **2–4**, 1–7 (2016).
3. Chancellor, J., Scott, G. & Sutton, J. Space Radiation: The Number One Risk to Astronaut Health beyond Low Earth Orbit. *Life* **4**, 491–510 (2014).
4. Guetersloh, S. et al. Polyethylene as a radiation shielding standard in simulated cosmic-ray environments. *Nucl. Instruments Methods Phys. Res. Sect. B Beam Interact. Mater. Atoms*. **252**, 319–332 (2006).
5. Kodaira, S. et al. Verification of shielding effect by the water-filled materials for space radiation in the International Space Station using passive dosimeters. *Adv. Sp Res.* **53**, 1–7 (2014).
6. Naito, M. et al. Applicability of composite materials for space radiation shielding of spacecraft. *Life Sci. Sp Res.* **31**, 71–79 (2021).
7. Naito, M. et al. Investigation of shielding material properties for effective space radiation protection. *Life Sci. Sp Res.* **26**, 69–76 (2020).
8. Al Zaman, M. A. & Kunja, L. A. Effectiveness of radiation shields constructed from Martian regolith and different polymers for human habitat on Mars using MULASSIS/GEANT4 and OLTARIS. *AIP Adv.* **13**, 85108 (2023).
9. Kunja, L. A., Yi, Y., Kim, E., Sohn, J. & Jung, J. Performance of hydrogen-rich materials in combination with lunar regolith for shielding against GCR, albedo, and SPEs on the surface of the moon studied using MULASSIS. *AIP Adv.* **15**, 125310 (2025).
10. Kunja, L. A., Kim, E., Yi, Y., Sohn, J. & Jung, J. Capability of lunar regolith with hydrogenous materials as shielding material against GCR and SPE on the surface of Moon studied using OLTARIS. *Adv. Sp Res.* https://doi.org/10.1016/j.asr.2025.06.059 (2025).
11. Weiss, P. et al. Advanced Materials for Future Lunar Extravehicular Activity Space Suit. *Adv. Mater. Technol.* **5**, 2000028 (2020).
12. Thibeault, S. et al. Radiation Shielding Materials Containing Hydrogen, Boron, and Nitrogen: Systematic Computational and Experimental Study-Phase I. NIAC FINAL REPORT. (2012).
13. Ryu, K. H. et al. Spacesuit Textiles from Extreme Fabric Materials: Aromatic Amide Polymer and Boron Nitride Nanotube Composite Fiber for Neutron Shielding and Thermal Management. *Adv Fiber Mater* **6**, (2024).
14. ESA. SPENVIS webpage. (2024). https://www.spenvis.oma.be/
15. Lei, F. et al. MULASSIS: A Geant4-based multilayered shielding simulation tool. *IEEE Trans. Nucl. Sci.*49 I, 2788–2793 (2002).

16. Carrier, J. F., Archambault, L., Beaulieu, L. & Roy, R. Validation of GEANT4, an object-oriented Monte Carlo toolkit, for simulations in medical physics. *Med. Phys.* **31**, 484–492 (2004).
17. Simpson, J. A. Elemental and Isotopic Composition of the Galactic Cosmic Rays. *Annu. Rev. Nucl. Part. Sci.* **33**, 323–382 (1983).
18. Slaba, T. C. et al. Validated space radiation exposure predictions from earth to mars during Artemis-I. *npj Microgravity*. **11**, 6 (2025).
19. Ehresmann, B. et al. Charged particle spectra obtained with the Mars Science Laboratory Radiation Assessment Detector (MSL/RAD) on the surface of Mars. *J. Geophys. Res. Planet*. **119**, 468–479 (2014).
20. Naito, M., Kusano, H. & Kodaira, S. Global dose distributions of neutrons and gamma-rays on the Moon. *Sci. Rep.* **13**, 13275 (2023).
21. Bernabeu, J. & Casanova, I. Geant4-based radiation hazard assessment for human exploration missions. *Adv. Sp Res.* **40**, 1368–1380 (2007).

Figures

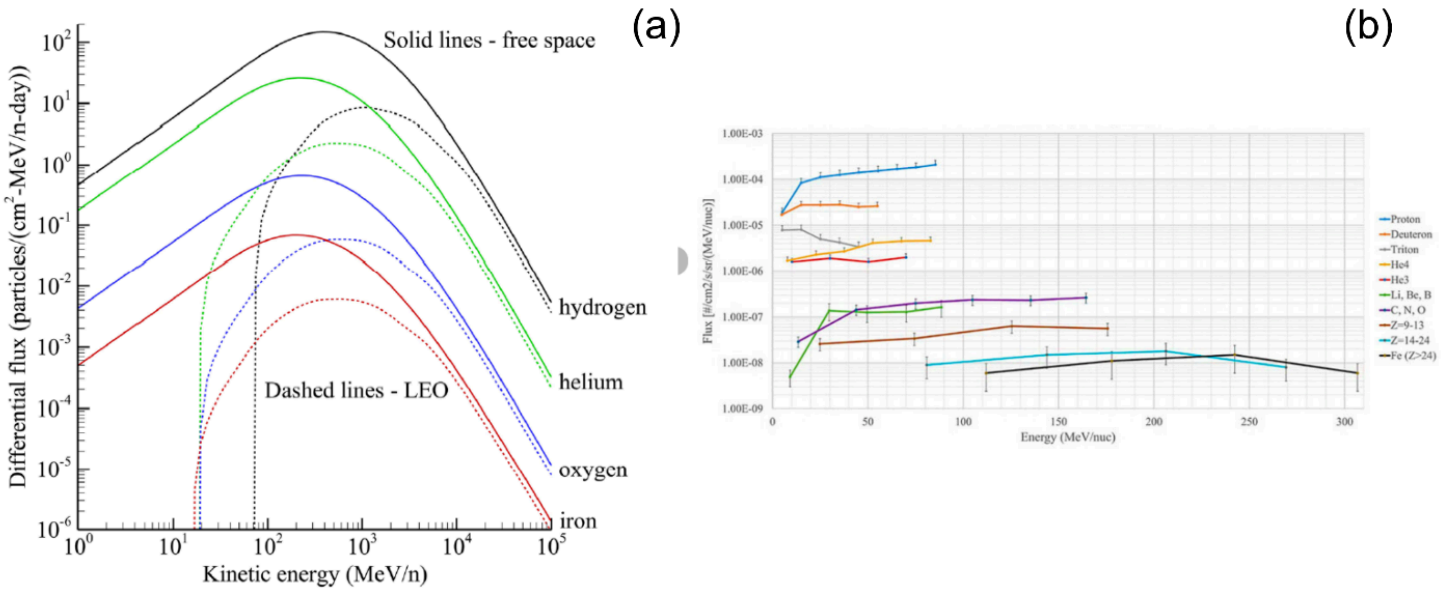

Figure 1

Radiation models used in the simulations. (a) GCR particle fluxes for H, He, O, and Fe, in free space, and (b) shows particle flux for GCR protons, He, and CNO on the Martian surface. The graph in (a) is taken from reference [18], which is published under the Creative Commons Attribution 4.0 International License. The graph in (b) is adapted from the reference [19]. Copyright 2014 AGU, which was published by the American Geophysical Union under the Creative Commons license

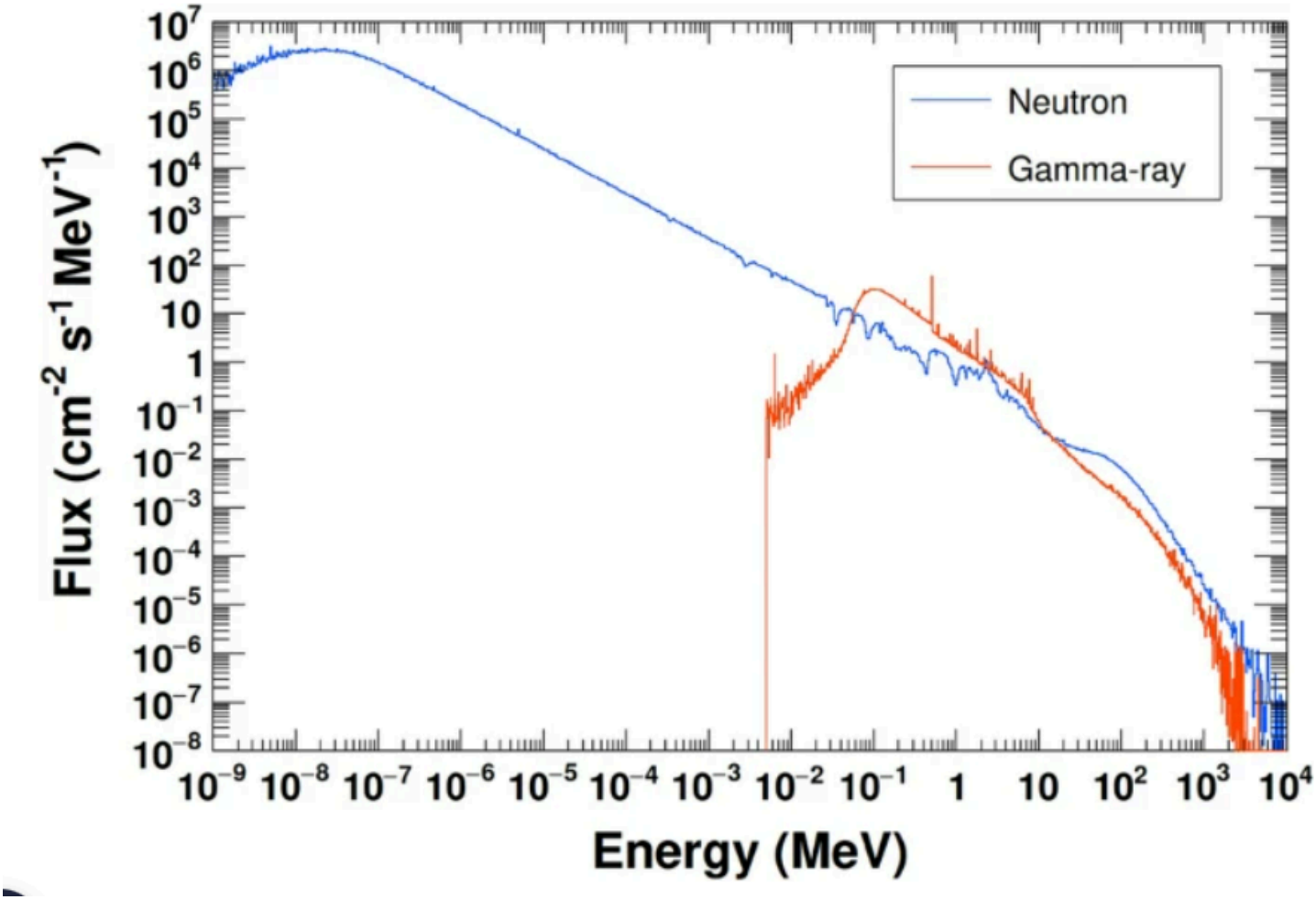

Figure 2

Radiation models used in the simulations. Secondary neutron and secondary gamma radiation on the Moon. The graph is taken from reference [20], which is published under the Creative Commons Attribution 4.0 International License

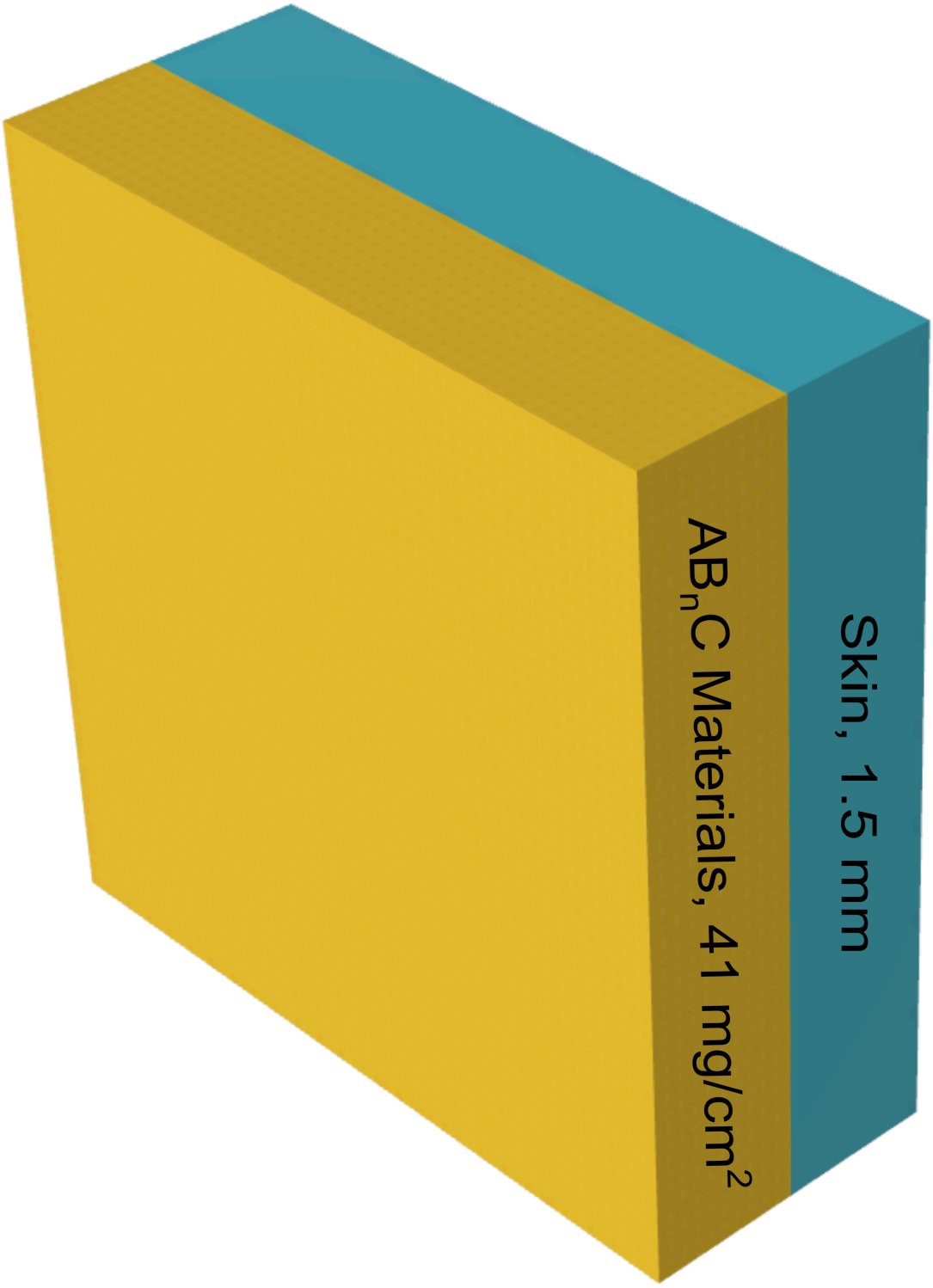

Figure 3

MULASSIS simulation setup. An angle view of the MULASSIS/GEANT-4 simulation system. In the AB_nC materials area is indicated by the first yellow region (0.41 mg/cm^2). The following blue layer (1.5 mm) denotes the skin materials where the absorbed radiation is calculated. A lower absorbed dose in the skin layer means, therefore better shielding by the tested material. The thicknesses of the different AB_nC materials were adjusted to achieve the same areal density across all materials.

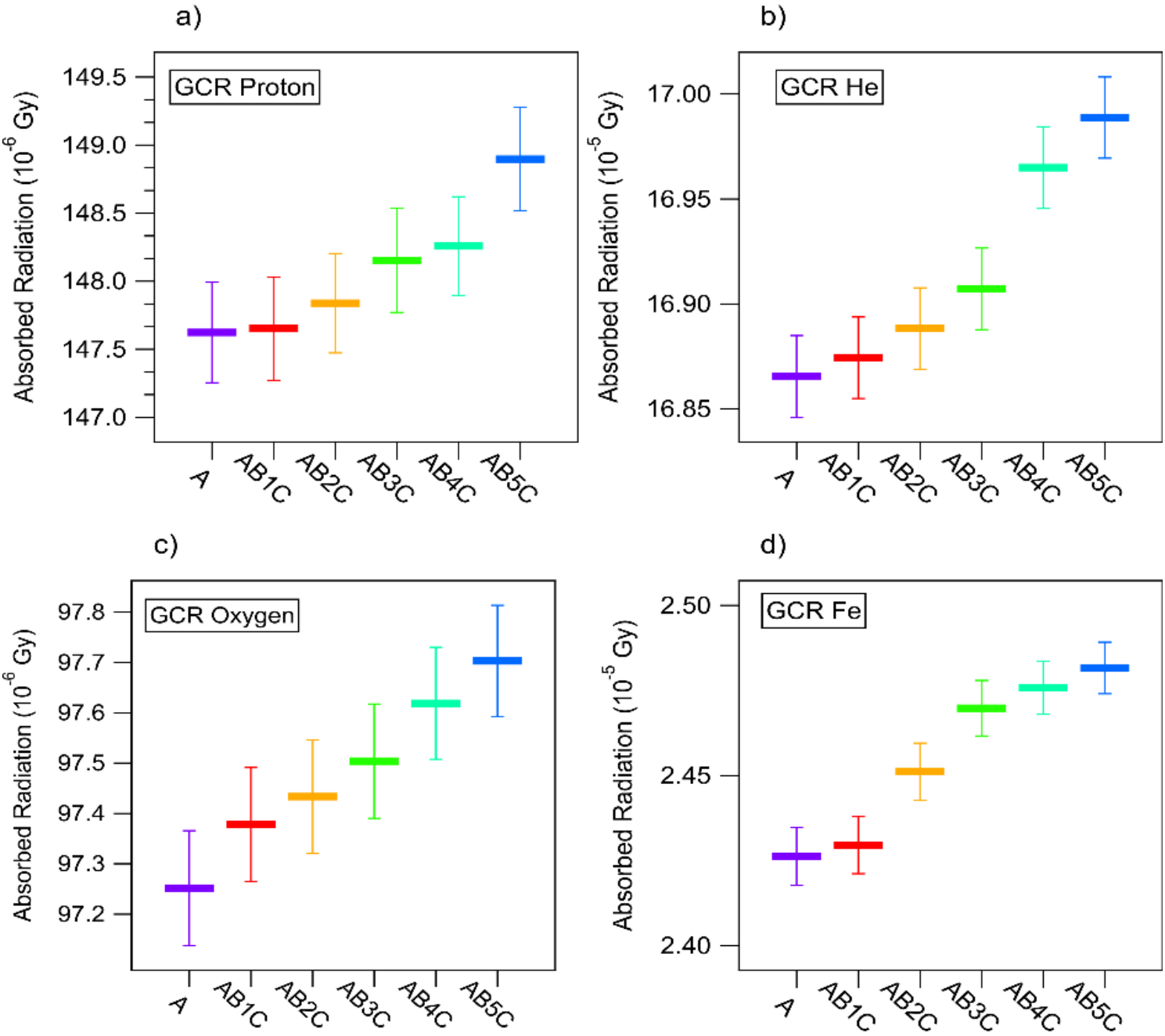

Figure 4

Shielding effect of different materials for the four individual parts of the GCR in space. a) proton radiation, b) He radiation, c) oxygen radiation, d) Fe radiation. The shielding model included a 0.41 mg/cm^2 slab, shown materials. The materials and colors are A (purple), AB_1C (red), AB_2C (yellow), AB_3C (green), AB_4C (cyan), and AB_5C (blue) on 1.5 mm of skin material. The simulations were performed in MULASSIS

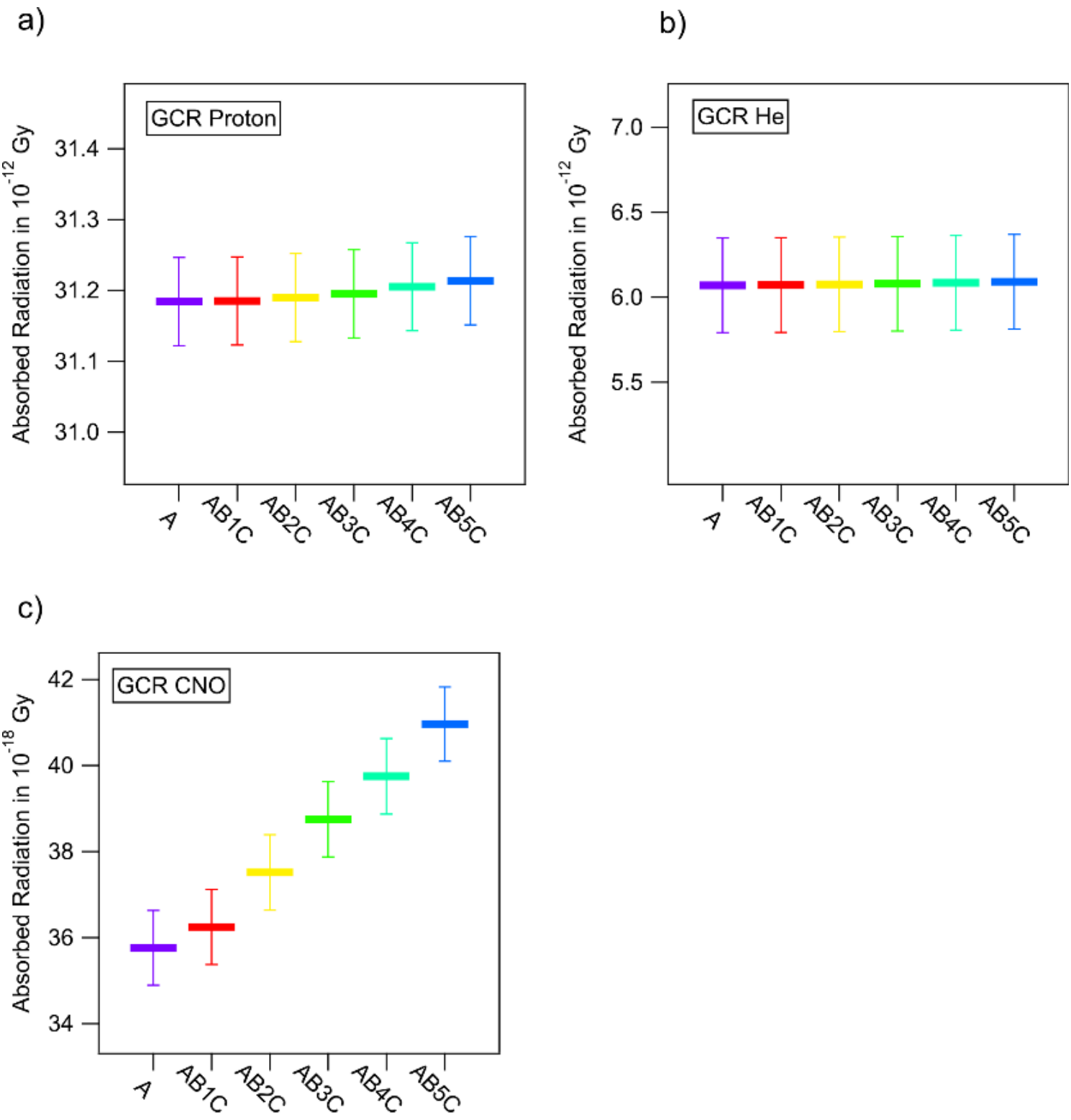

Figure 5

Shielding effect of different materials for the three individual parts of the GCR on the Martian surface. a) proton radiation, b) He radiation, c) CNO radiation. The shielding model included a 0.41 mg/cm^2 slab of the shown materials. The materials and colors are A (purple), AB_1C (red), AB_2C (yellow), AB_3C (green), AB_4C (cyan), and AB_5C (blue) on 1.5 mm of skin materials. The simulations were performed in MULASSIS

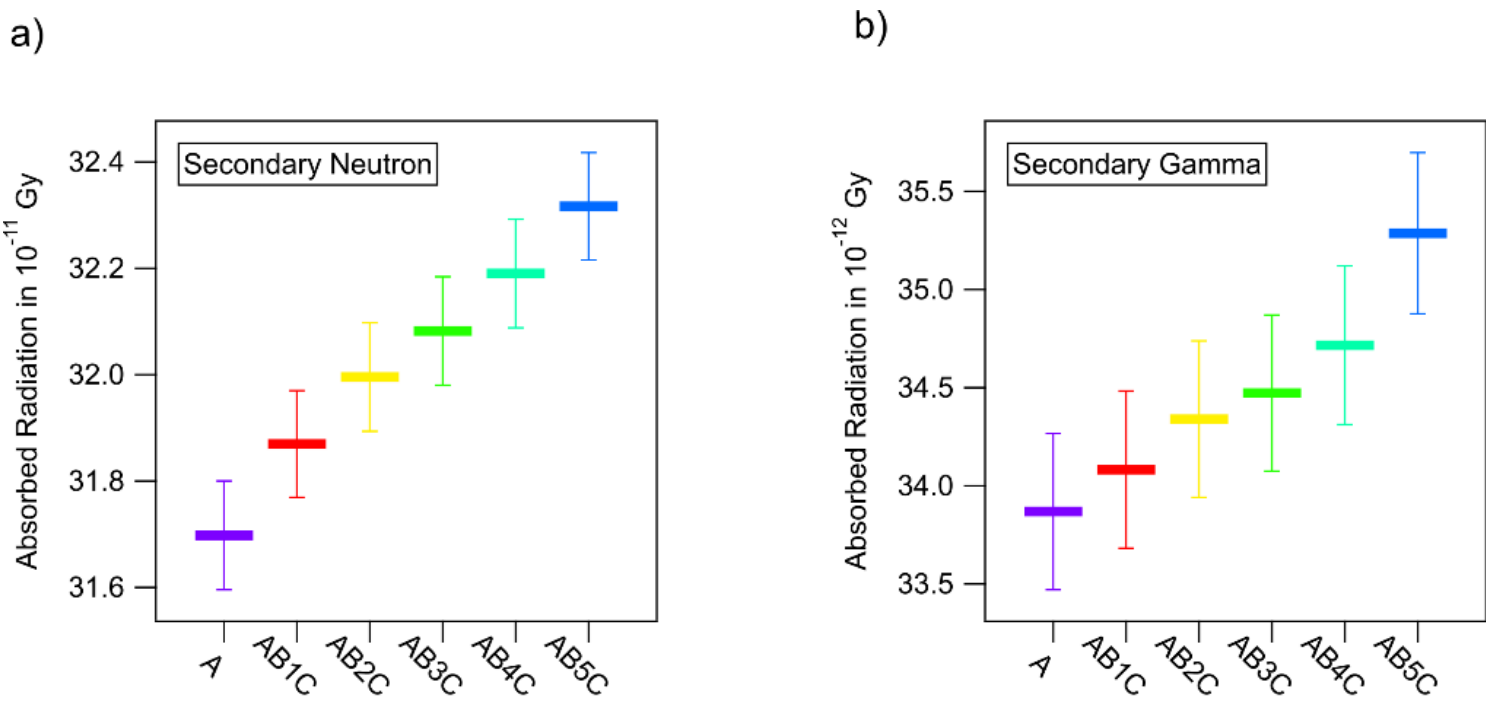

Figure 6

Shielding effect of different materials for two individual parts of the secondary radiation on the surface of the Moon. a) Secondary Neutron radiation, b) Secondary Gamma radiation on the lunar surface. The shielding model included a 0.41 mg/cm^2 slab of the shown materials. The materials and colors are A (purple), AB_1C (red), AB_2C (yellow), AB_3C (green), AB_4C (cyan), and AB_5C (blue) on 1.5 mm of skin materials. The simulations were performed in MULASSIS

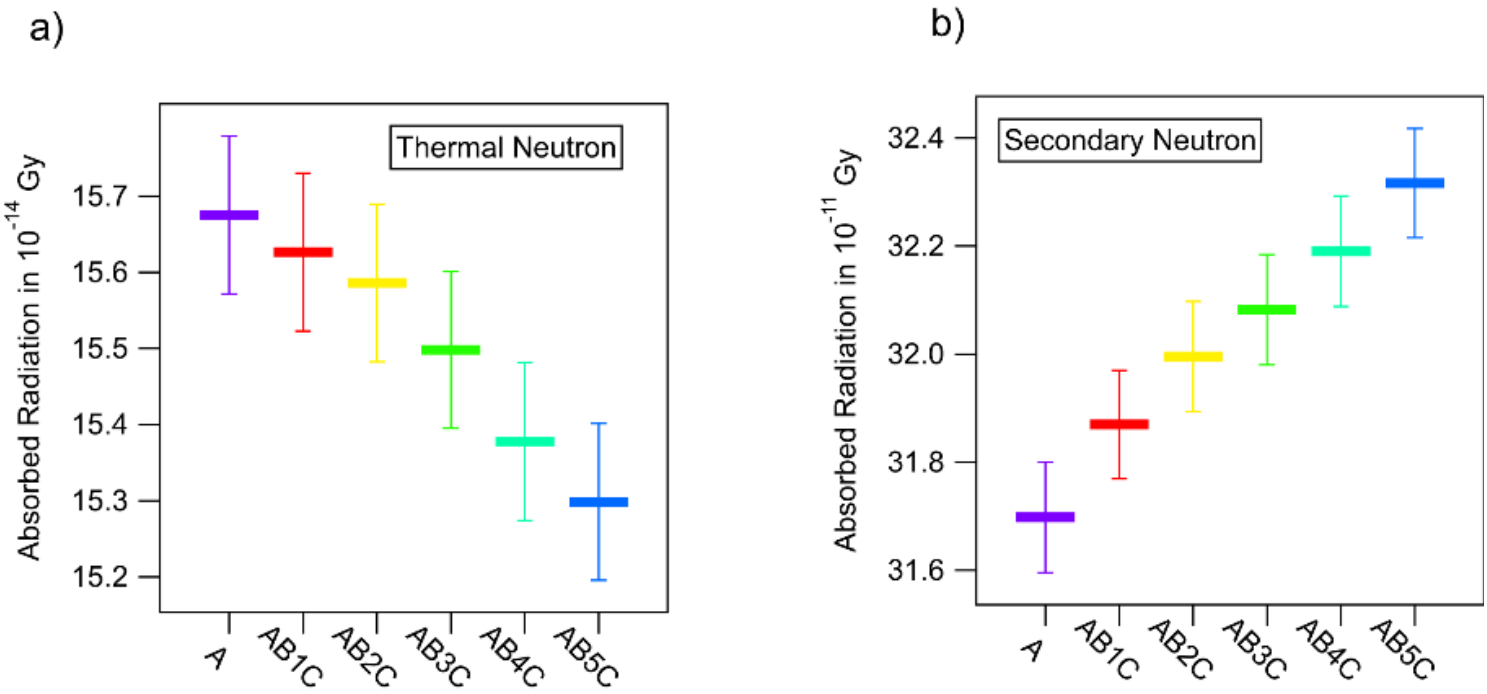

Figure 7

Shielding effect of different materials for the two individual parts of the secondary neutron radiation on the surface of the Moon. a) Thermal Neutron radiation, b) Secondary Neutron radiation. The shielding model included a 0.41 mg/cm^2 slab of the shown materials. The materials and colors are A (purple), AB_1C (red), AB_2C (yellow), AB_3C (green), AB_4C (cyan), and AB_5C (blue) on 1.5 mm of skin materials. The simulations were performed in MULASSIS

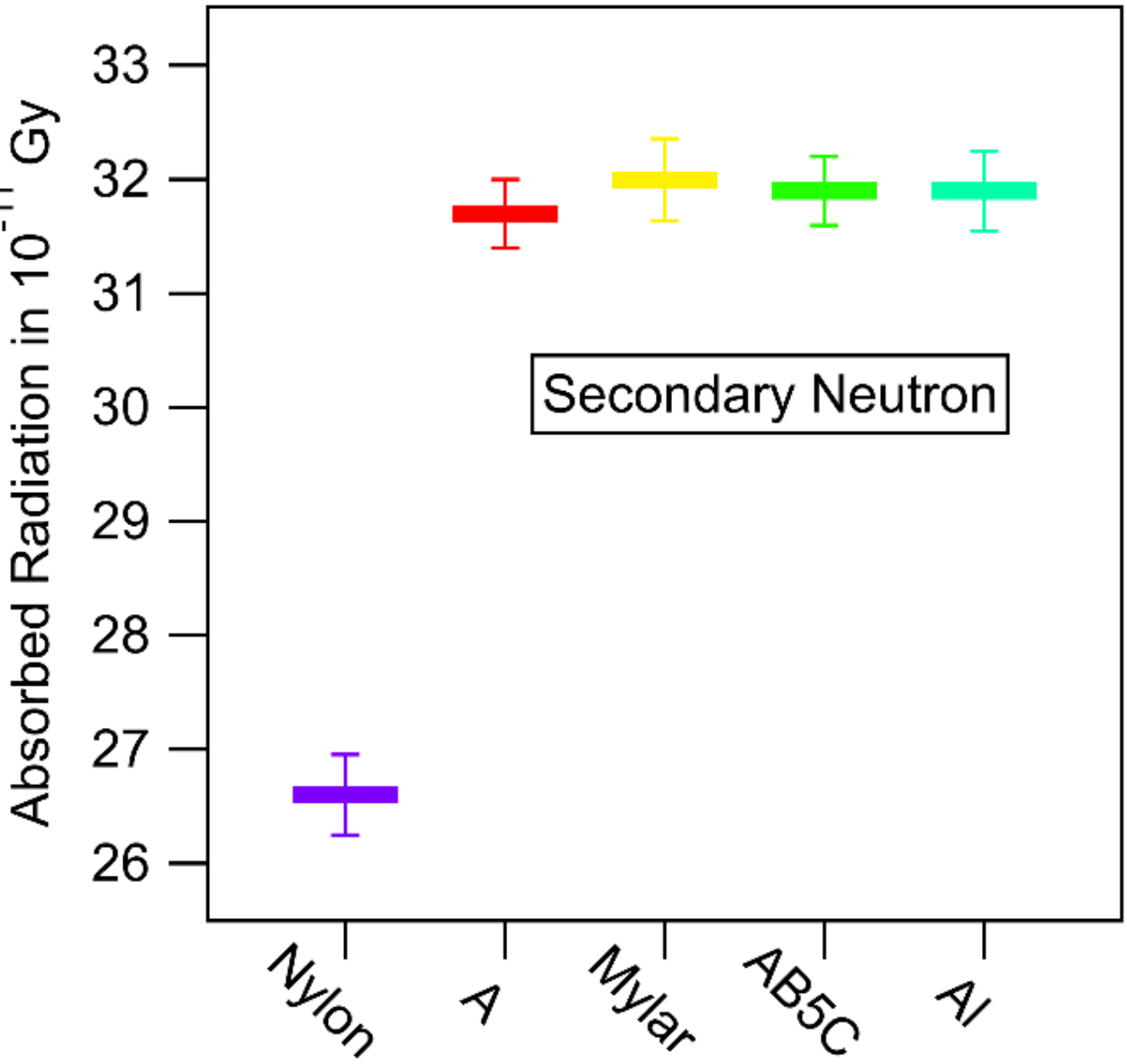

Figure 8

Shielding effect of different materials for the secondary radiation, Secondary Neutron radiation on the surface of the Moon. The shielding model included a 0.41 mg/cm^2 slab of the shown materials. The materials and colors are Nylon (purple), A (red), Mylar (yellow), AB_5C (green), and Al (cyan) on 1.5 mm of skin material. The simulations were performed in MULLASSIS